The American Journal of Human Genetics, Volume *105*

Supplemental Data

NCALD Antisense Oligonucleotide Therapy in Addition to Nusinersen further Ameliorates Spinal Muscular Atrophy in Mice

Laura Torres-Benito, Svenja Schneider, Roman Rombo, Karen K. Ling, Vanessa Grysko, Aaradhita Upadhyay, Natalia L. Kononenko, Frank Rigo, C. Frank Bennett, and Brunhilde Wirth

SUPPLEMENTAL FIGURES AND LEGENDS

A

Ncald ex 5-6 PPS	Length (bp)	Sequence
***Ncald* ex 5-6P**	28	TCCGCCAGATGGATACCAATAGAGATGG
***Ncald* ex 5-6F**	21	TGCCTGAAGATGAATCAACCC
***Ncald* ex 5-6R**	19	AGGAGACGCACAATGGATG

B

IONIS #	Name	Chemistry	Results in neonatal injected mice
676626	Control-ASO	MOE-gapmer, mixed backbone	None of Control-ASO injected mice died
673672	*Ncald*-ASO1	MOE-gapmer, mixed backbone	30% of mice died after injection with *Ncald*-ASO1
673663	*Ncald*-ASO2	MOE-gapmer, mixed backbone	50% of mice died after injection with *Ncald*-ASO2
673756	*Ncald*-ASO3	MOE-gapmer, mixed backbone	None of *Ncald*-ASO3 injected mice died

C

IONIS #	Name	Length (bp)	Sequence
676626	Control-ASO	20	GTTTTCAAATACACCTTCAT
673672	*Ncald*-ASO1	20	AACACTTAATTTGGTCTGCA
673663	*Ncald*-ASO2	20	TGGCATTTGAATATGTGTTT
673756	*Ncald*-ASO3	20	GTGGTTCTTGTTTTACAGGA

Figure S1: ASO sequences, design and optimization.

(A) Prime probe sets used in the qRT-PCR to amplify mouse *Ncald* and evaluate downregulation in brain and spinal cord.

(B) Selected ASOs for neonatal injection and dosage optimization.

(C) Selected ASO sequences for neonatal injection and dosage optimization. bp = base pairs.

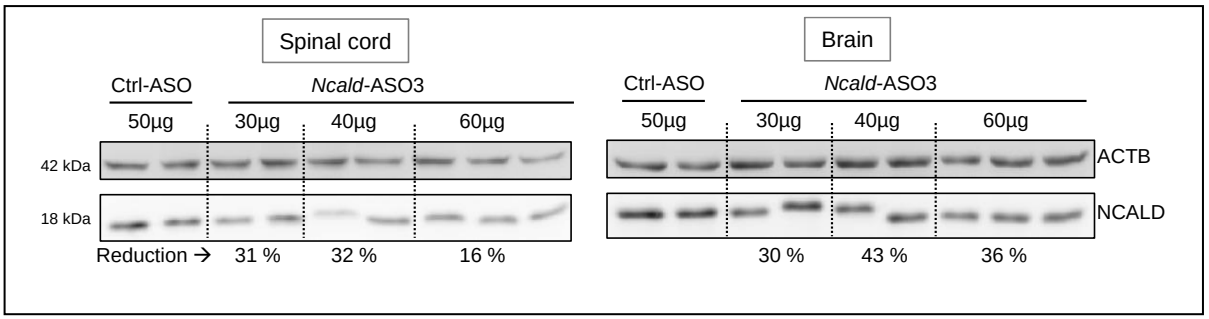

Figure S2: *Ncald*-ASO3 dosage optimization for i.c.v. injections in neonatal mice. Western blot analysis showing NCALD downregulation efficiency in the spinal cord and the brain of P10 *Ncald*-ASO3 HET and SMA animals intracerebroventicularly (i.c.v.) injected on postnatal day 2 (P2) with either 50 µg of Ctrl-ASO or 30, 40, or 60 µg of *Ncald*-ASO3. Numbers at the bottom indicate NCALD protein levels in *Ncald*-ASO3-treated animals normalized to the Ctrl-ASO injected animals in percentages. Numbers on the left indicate respective band size in kDa. ACTB = loading control. Unpaired, two-tailed Student´s *t*-test; * $P < 0.05$, *** $P < 0.001$.

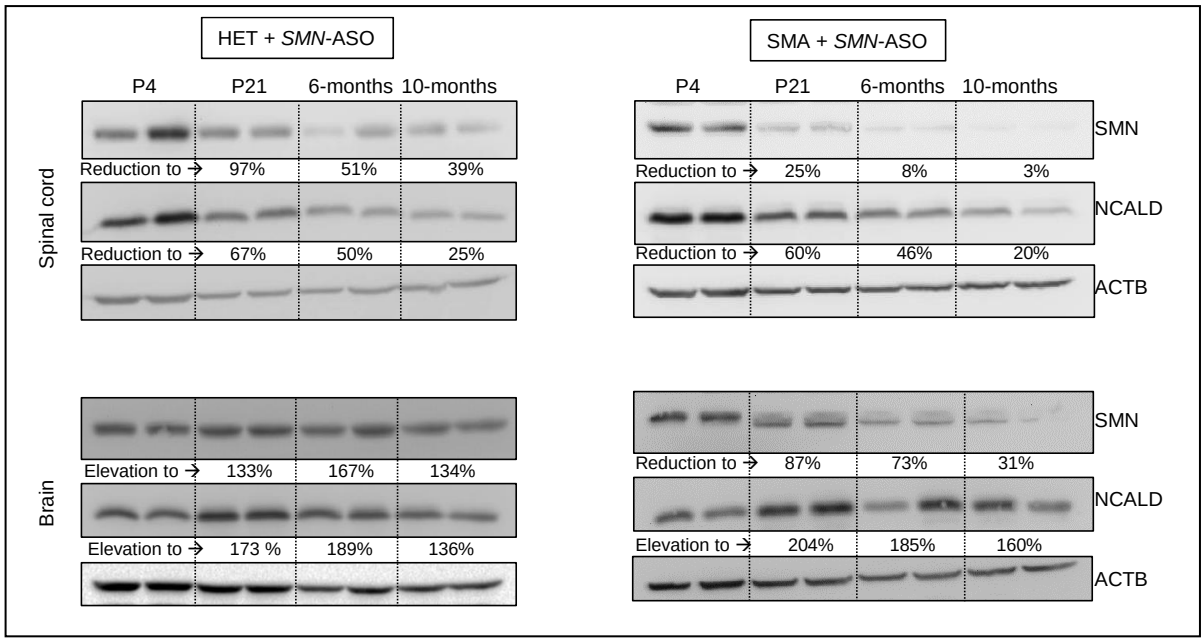

Figure S3: NCALD is naturally downregulated during adulthood in spinal cord.

Western blots of spinal cord and brain from HET and SMA animals injected with a single low-dose of 30 µg *SMN*-ASO: Spinal cord and brain samples were taken from mice at the indicated time points P4, P21, 6 months and 10 months to analyze the time course behavior of SMN and NCALD protein levels. Note that in contrary to the brain, NCALD levels in the spinal cord in both HET and SMA animals are decreasing during the adulthood. ACTB= loading control.

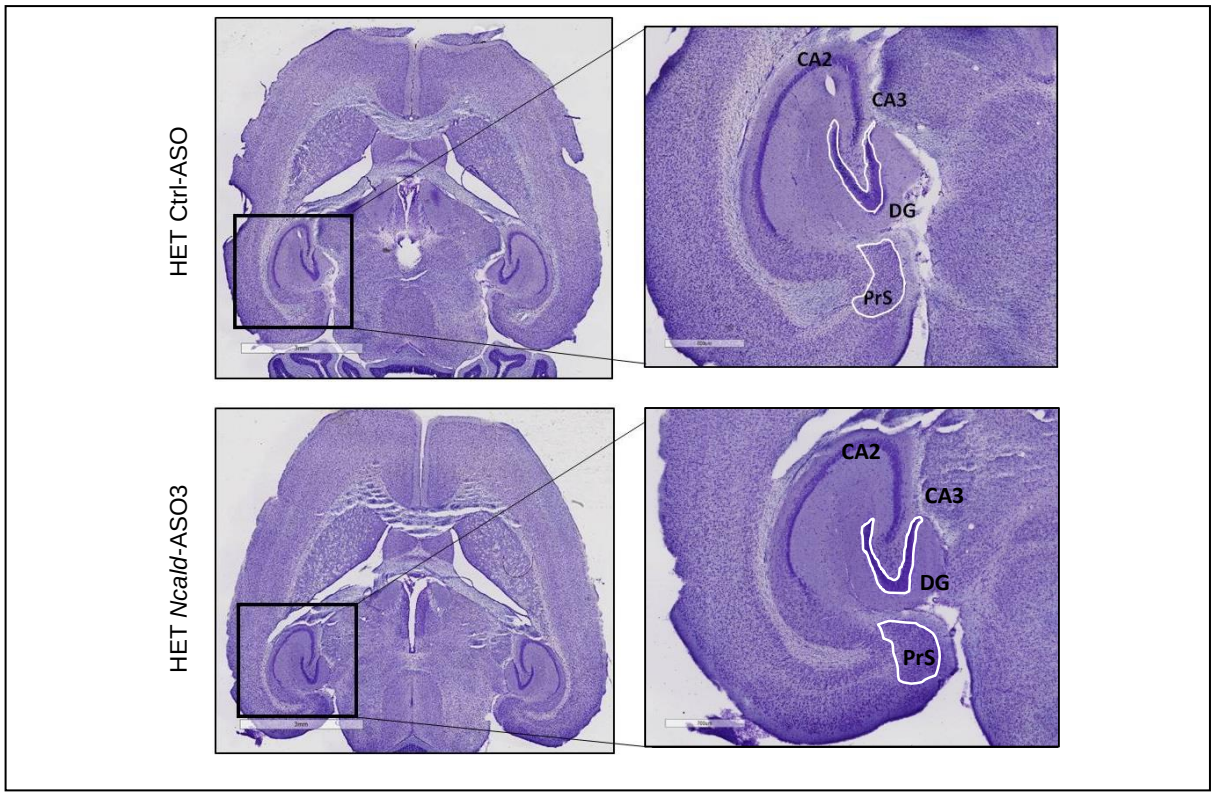

Figure S4: Brain morphology in adult mice upon *Ncald*-ASO3 treatment.

Horizontal sections of brains from 4 months **(A)** HET Ctrl-ASO and **(B)** HET *Ncald*-ASO3**.** Cresyl violet staining was performed to visualize the brain gross-morphology. CA2 and CA3, cornu ammonis hippocampal areas; DG, dentate gyrus; PrS, presubiculum. Scale bars = 100 µm.

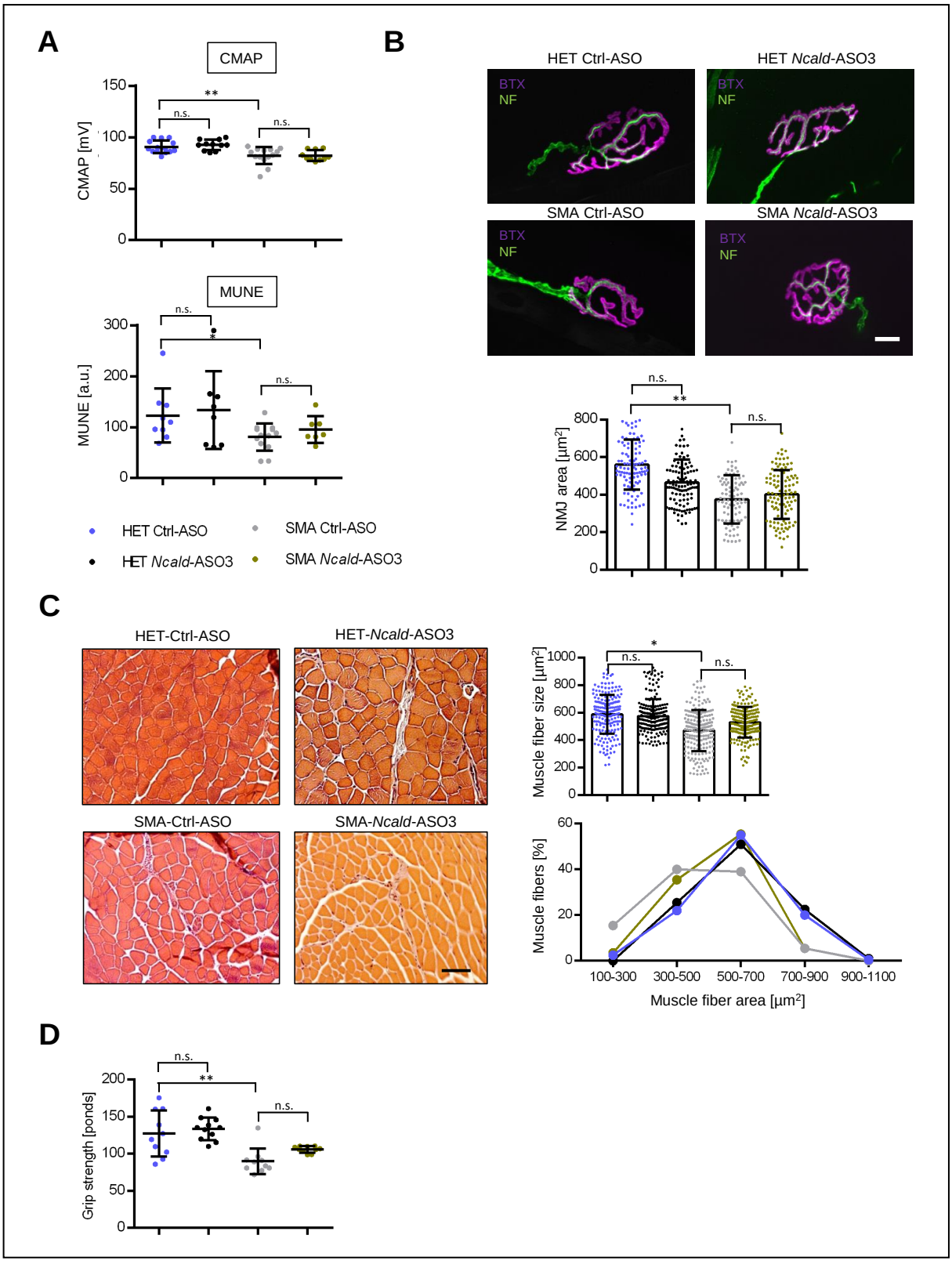

Figure S5: SMA hallmarks studied in HET and SMA animals co-injected with *SMN*-ASO and either control or *Ncald*-ASO3.

(A) Dot plot of CMAP amplitudes and MUNE values in HET and SMA animals at 3 months. Animals used for CMAP: HET Ctrl-ASO n=14; HET *Ncald*-ASO3 n=11; SMA Ctrl-ASO n=14; SMA *Ncald*-ASO3 n=10. MUNE: HET Ctrl-ASO n=9; HET *Ncald*-ASO3 n=8; SMA Ctrl-ASO n=13; SMA *Ncald*-ASO3 n=7, Color legend displayed at the bottom. For all analyses, ordinary one-way ANOVA with Tukey posthoc test for multiple comparisons was applied. n.s. = not significant, * $P < 0.05$, ** $P < 0.01$, *** $P < 0.001$

(B) Representative NMJ images in HET and SMA animals at 3 months showing postsynaptic NMJ region stained with bungarotoxin (BTX, magenta) and presynaptic nerve with neurofilament (NF; green). Graphs on the right show single dot plot values of NMJ areas of all grouped animals with mean ± SD. Quantification of maturity of NMJs with mean values of mice per group ± SD. Statistics was performed with mean values of animals per group. N = 4 animals per group, 30-55 NMJs per animal. Ordinary one-way ANOVA with Tukey posthoc test for multiple comparisons; n.s. = not significant, * $P < 0.05$, ** $P < 0.01$. Scale bars = 10 µm.

(C) Representative pictures and quantifications of haematoxylin and eosin-stained gastrocnemius (GC) muscle at 3 months. Graphs on the right show single dot plot values of GC areas of all grouped animals with mean ± SD (N = 4 animals per genotype, n = 50 fibers/mouse). For visualization, muscle fibres were grouped according to the area intervals of 100 μm^2. Ordinary one-way ANOVA with Tukey posthoc test for multiple comparisons; n.s. = not significant, * $P < 0.05$, ** $P < 0.01$. Scale bars = 50 µm.

(D) Dot plot quantification of grip strength at 6-months. Single values of each animal are shown as mean ± SD. Note that at 3 months SMA *Ncald*-ASO3 mice show stronger grip strength abilities compared to SMA Ctrl-ASO injected mice. Number of animals used are: HET Ctrl-ASO N = 10, HET *Ncald*-ASO3 N = 11, SMA Ctrl-ASO N = 10, SMA *Ncald*-ASO3 N = 10. Ordinary one-way ANOVA with Tukeys posthoc test for multiple comparisons. n.s. = not significant, * $P < 0.05$, ** $P < 0.01$, n.s. = not significant

SUPPLEMENTAL MATERIAL AND METHODS

Mouse model and genotyping

The Taiwanese SMA mice (FVB.Cg-Tg(SMN2)2Hung *Smn1*^{tm1Hung}/J, stock number 005058) were purchased from Jackson Laboratory [1]. Originally, the purchased SMA mice were on a pure FVB/N background; however, we used an additionally mouse line which has been previously backcrossed for >7 generations with C57BL6/N wildtype to obtain a pure C57BL6/N background [2]. An intermediate mouse model was produced crossing *Smn*$^{ko/ko}$*; SMN2*$^{tg/tg}$ mice on FVB background with *Smn*$^{ko/wt}$ on C57Bl6/N background to obtain both *Smn*$^{ko/wt}$*; SMN2*$^{tg/0}$ (named as HET) and *Smn*$^{ko/ko}$*; SMN2*$^{tg/0}$ (named as SMA) mixed$_{50}$ litters (50% FVB/N: 50%C57BL6/N) [3]. Primers used for litters genotyping were as follows: SmnKOfw: 50-ATAACACCACCACTCTTACTC-30; SmnKOrev1: 50-AGCCTGAAGAACGAGATCAGC-30; SmnKOrev2: 50-TAGCCGTGATGCCATTGTCA-30. A mild SMA mouse model was produced by suboptimal subcutaneous injection of severe SMA mice (50% FVB: 50% C57BL6/N) at P1 with 30 µg of SMN-ASO (Ionis Pharmaceuticals®) using a microliter syringe (Hamilton)[3].

Antisense oligonucleotides (ASOs) design

IONIS Pharmaceuticals (Carlsbad, California) designed 40 antisense oligonucleotides (ASOs) to achieve *Ncald* downregulation in the CNS. Synthesis and purification of all chemically modified oligonucleotides were performed as previously described [4]. The 5-10-5 2'-O-methoxyethyl (MOE) gapmer ASOs were 20 nucleotides in length, comprising five 2' MOE modified nucleotides on 5' and 3' wings flanking the central gap segment of ten 2'-deoxyribonucleotides. Internucleotide linkages are phosphorothioate interspersed with phosphodiester, and all cytosine residues are 5'-methylcytosines. 22 MOE gapmer ASOs targeting mouse *Ncald* efficiently suppressed *Ncald* mRNA expression in primary neuronal cultures were identified. Subsequently those 22 ASOs were tested for target reduction in the CNS of adult mice.

ASOs injection and optimization

A control-ASO (#676626) and the three *Ncald*-ASOs which achieved the highest *Ncald* KD in adult injected mice were chosen for future tolerability test: #673663 and #673672 referred to as *Ncald*-ASO1 and *Ncald*-ASO2, respectively. As those, but the control ASO showed toxicity in neonatal injected mice, we also tested the #673756 (named as *Ncald*-ASO3). Neonatal mice were i.c.v. injected in the right hemisphere close to the confluence of the sinuses with different ASOs concentration (ranging from 30 to 100 µg) [5]. All ASOs were diluted in sterile PBS and the concentration of the working solution in each case was calculated using photometric density (AD260) to administer 1.5 µl in the brain (1 µl of the ASO + 0.5 µl of 0.05% w/v trypan blue in PBS). All mice were blinded injected.

Western blot

Brain and spinal cords were dissected from experimental mice and lysed in RIPA buffer (Sigma) containing protease inhibitors (Complete Mini, Roche). Following primary antibodies were used: anti-beta-actin HRP-conjugated (A5316, Sigma), anti-SMN (mouse, MANSMA7, Hybridoma Bank; 610646, BD Biosciences), and anti-NCALD (rabbit, 12925-1-AP, Proteintech). Signal was detected with the corresponding HRP conjugated-secondary antibodies (α-mouse, Dianova, 115-035-003; α-rabbit, Cell signalling, 7074) and Chemiluminescence reagent (Thermo Scientific) according to manufacturer´s protocol.

Motoric abilities

To analyze the motoric ability of the animals, the grip strength [6] was performed with 3- and 6-month-old mice via the Grip Strength Meter (TSE System). Muscle force was recorded in pounds.

Electrophysiological biomarkers

Compound muscle action potential (CMAP) and motor unit number estimation (MUNE) were recorded to analyze motor improvement as previously described [7-9]. Mice were placed in a thermostatic warming plate at 37°C with continuous inhaled isofluorane anesthesia (1 L/min O_2 flow rate, 5% induction and 1.5-2% maintenance). Stimulation electrode was positioned in the close vicinity of the sciatic nerve and the active recording electrode was placed on the proximal gastrocnemius. UltraPro S100 from Natus Neurology components were used for the electrophysiology measurements. Nerve was stimulated with square-wave pulses of 50 μs duration and 3-10 mA amplitude to record the supramaximal response of the muscle. CMAP was expressed in mV as the peak-to-peak amplitude of the response. To estimate the motor unit number (MUNE) ten subsequent increments from the initial response were recorded and calculated according to [7]

Immunohistochemistry of NMJ

We performed the NMJ characterization and analysis in the *Transversus abdominis* muscle. Muscles from all genotypes and treated mice were dissected as previously described [10] and fixed with 4 % PFA for 20 minutes. Following primary antibodies were incubated over night at 4 °C: rabbit anti-NF-L (Cell Signalling, C28E10). Postsynaptic AChR were stained with BTX-568 (Invitrogen, B13423) which was incubated at room temperature together with secondary antibodies: rabbit AlexaFluor-488 (Invitrogen, A21206) and mouse AlexaFluor-647 (Invitrogen, A31571). Finally, muscles were mounted on slides with Prolong Gold™ antifade reagent (Invitrogen, P36934). Quantification of NMJ size and maturity was performed using ImageJ [3]. NMJ maturity was evaluated as followed: NMJs exhibiting ≥3 perforations were evaluated as mature, NMJs with <3 perforations as immature [8].

Histology

To quantify muscle fiber size on the *gastrocnemius* muscle dissection of the whole muscle was carried out. Muscles were infiltrated and embedded in paraffin and sectioned as previously described [2]. Hematoxilin (SIGMA-ALDRICH, MHS32) and eosin (ScyTek Laboratories, EYQ999) (H&E) staining was performed to visualize the fiber diameter.

For morphological analysis, a whole brain from 4-month-old HET Ctrl-ASO and HET *Ncald*-ASO3-treated mice was dissected after transcardial perfusion with 4% PFA as previously described [11]. Brain tissue and spinal cords were processed for cryocutting. Brains were cut in 10 µm slices (Cryostat, Leica). A Cresyl violet (SIGMA, C5042) staining was performed in order to visualize the brain morphology.

Image acquisition and analysis

Fluorescence images from NMJs and spinal cords were acquired with a Zeiss microscope (AxioImager.M2) supplied with the Apotome.2 system which mimics confocality. Images were acquired as Z-stacks with 40X and 63X-oil immersion objective (1.4 NA). Quantitative analysis was executed with ZEN software (Zeiss) and Fiji software. For NMJ maturity analysis, NMJs were categorized as mature with > 3 perforations and as immature with < 3 perforations. Bright field images for muscle fiber analysis were acquired with Zeiss microscope (Axioskop.2) equipped with AxioCamICc1 and 20X objective. Brain sections were imaged with Leica Slide Scanner (SCN400) and morphological analysis was executed with OMERO.insight_64. Image acquisition and analysis were performed blinded.

Statistics

Statistical analyses were performed in GraphPad Prism 6. Unpaired, two tailed Student's t-tests and one-way ANOVA statistics tests with Tukeys posthoc test for multiple comparisons were performed. Levels of statistical significance were given as follows: *$p \leq 0.05$, **$p \leq 0.01$,

and ***p ≤ 0.001. Specific tests, sample size, data representation and p-values are indicated in figure legends.

Study approval

Mice care and experiments were performed according to the institutional animal care committee guidelines and approved by LANUV NRW (Landesamt für Natur, Umwelt und Verbraucherschutz NRW) under the reference numbers 84-02.04.2014.A126.

SUPPLEMENTAL REFERENCES

1. Hsieh-Li, H.M., Chang, J.G., Jong, Y.J., Wu, M.H., Wang, N.M., Tsai, C.H., and Li, H. (2000). A mouse model for spinal muscular atrophy. Nat Genet 24, 66-70.
2. Ackermann, B., Krober, S., Torres-Benito, L., Borgmann, A., Peters, M., Hosseini Barkooie, S.M., Tejero, R., Jakubik, M., Schreml, J., Milbradt, J., et al. (2013). Plastin 3 ameliorates spinal muscular atrophy via delayed axon pruning and improves neuromuscular junction functionality. Hum Mol Genet 22, 1328-1347.
3. Riessland, M., Kaczmarek, A., Schneider, S., Swoboda, K.J., Lohr, H., Bradler, C., Grysko, V., Dimitriadi, M., Hosseinibarkooie, S., Torres-Benito, L., et al. (2017). Neurocalcin Delta Suppression Protects against Spinal Muscular Atrophy in Humans and across Species by Restoring Impaired Endocytosis. Am J Hum Genet 100, 297-315.
4. Swayze, E.E., Siwkowski, A.M., Wancewicz, E.V., Migawa, M.T., Wyrzykiewicz, T.K., Hung, G., Monia, B.P., and Bennett, C.F. (2007). Antisense oligonucleotides containing locked nucleic acid improve potency but cause significant hepatotoxicity in animals. Nucleic Acids Res 35, 687-700.
5. Glascock, J.J., Osman, E.Y., Coady, T.H., Rose, F.F., Shababi, M., and Lorson, C.L. (2011). Delivery of therapeutic agents through intracerebroventricular (ICV) and intravenous (IV) injection in mice. J Vis Exp.
6. El-Khodor, B.F., Edgar, N., Chen, A., Winberg, M.L., Joyce, C., Brunner, D., Suarez-Farinas, M., and Heyes, M.P. (2008). Identification of a battery of tests for drug candidate evaluation in the SMNDelta7 neonate model of spinal muscular atrophy. Exp Neurol 212, 29-43.
7. Arnold, W.D., Sheth, K.A., Wier, C.G., Kissel, J.T., Burghes, A.H., and Kolb, S.J. (2015). Electrophysiological Motor Unit Number Estimation (MUNE) Measuring Compound Muscle Action Potential (CMAP) in Mouse Hindlimb Muscles. J Vis Exp.
8. Bogdanik, L.P., Osborne, M.A., Davis, C., Martin, W.P., Austin, A., Rigo, F., Bennett, C.F., and Lutz, C.M. (2015). Systemic, postsymptomatic antisense oligonucleotide rescues motor unit maturation delay in a new mouse model for type II/III spinal muscular atrophy. Proc Natl Acad Sci U S A 112, E5863-5872.
9. Janzen, E., Mendoza-Ferreira, N., Hosseinibarkooie, S., Schneider, S., Hupperich, K., Tschanz, T., Grysko, V., Riessland, M., Hammerschmidt, M., Rigo, F., et al. (2018).

CHP1 reduction ameliorates spinal muscular atrophy pathology by restoring calcineurin activity and endocytosis. Brain 141, 2343-2361.

10. Torres-Benito, L., Ruiz, R., and Tabares, L. (2012). Synaptic defects in spinal muscular atrophy animal models. Dev Neurobiol 72, 126-133.

11. Upadhyay, A., Hosseinibarkooie, S., Schneider, S., Kaczmarek, A., Torres-Benito, L., Mendoza-Ferreira, N., Overhoff, M., Rombo, R., Grysko, V., Kye, M.J., et al. (2019). Neurocalcin Delta Knockout Impairs Adult Neurogenesis Whereas Half Reduction Is Not Pathological. Front Mol Neurosci 12, 19.